




The improved dissolution performance of a post processing treated spray-dried crystalline solid dispersion of poorly soluble drugs

Siok-Yee Chan, Seok-Ming Toh, Nasir Hayat Khan, Yin-Ying Chung & Xin-Zi Cheah

To cite this article: Siok-Yee Chan, Seok-Ming Toh, Nasir Hayat Khan, Yin-Ying Chung & Xin-Zi Cheah (2016): The improved dissolution performance of a post processing treated spray-dried crystalline solid dispersion of poorly soluble drugs, Drug Development and Industrial Pharmacy, DOI: [10.3109/03639045.2016.1173054](https://doi.org/10.3109/03639045.2016.1173054)

To link to this article: <http://dx.doi.org/10.3109/03639045.2016.1173054>

 View supplementary material 

 Accepted author version posted online: 06 Apr 2016.
Published online: 24 Apr 2016.

 Submit your article to this journal 

 Article views: 16

 View related articles 

 View Crossmark data 

RESEARCH ARTICLE

The improved dissolution performance of a post processing treated spray-dried crystalline solid dispersion of poorly soluble drugs

Siok-Yee Chan, Seok-Ming Toh, Nasir Hayat Khan, Yin-Ying Chung and Xin-Zi Cheah

School of Pharmaceutical Sciences, Universiti Sains Malaysia, Penang, Malaysia

ABSTRACT

Context: Solution-mediated transformation has been cited as one of the main problems that deteriorate dissolution performances of solid dispersion (SD). This is mainly attributed by the recrystallization tendency of poorly soluble drug. Eventually, it will lead to extensive agglomeration which is a key process in reducing the dissolution performance of SD and offsets the true benefit of SD system. Here, a post-processing treatment is suggested in order to reduce the recrystallization tendency and hence bring forth the dissolution advantage of SD system.

Objectives: The current study investigates the effect of a post processing treatment on dissolution performance of SD in comparison to their performances upon production.

Methods: Two poorly soluble drugs were spray dried into SD using polyvinyl alcohol (PVA) as hydrophilic carrier. The obtained samples were post processing treated by exposure to high humidity, i.e. 75% RH at room temperature. The physical properties and release rate of the SD system were characterized upon production and after the post-processing treatment.

Results and discussion: XRPD, Infrared and DSC results showed partial crystallinity of the fresh SD systems. Crystallinity of these products was further increased after the post-processing treatment at 75% RH. This may be attributed to the high moisture absorption of the SD system that promotes recrystallization process of the drug. However, dissolution efficiencies of the post-treated systems were higher and more consistent than the fresh SD. The unexpected dissolution trend was further supported by the results intrinsic dissolution and solubility studies.

Conclusions: An increase of crystallinity in a post humidity treated SD did not exert detrimental effect to their dissolution profiles. A more stabilized system with a preferable enhanced dissolution rate was obtained by exposing the SD to a post processing humidity treatment.

ARTICLE HISTORY

Received 17 November 2015
Revised 24 March 2016
Accepted 27 March 2016
Published online 25 April 2016

KEYWORDS

Amorphous; ketoprofen; piroxicam; post treatment; PVA; solid dispersion

Introduction

The use of new techniques to improve the solubility, dissolution rate and bioavailability of the poorly water soluble drugs is of great importance in the development of medicines, particularly those administered orally. Various solubilization technologies have been developed including solid dispersions (SD), nanocrystals, cyclodextrin complexes and lipid formulations¹. Among these SD is one of the promising techniques in increase dissolution performances of drugs.

A solid dispersion refers to a dispersion of one or more active ingredients in an inert carrier or matrix at solid state. The drug can be molecularly dispersed, in amorphous particles as clusters or in crystalline particles². Many studies have shown that the preparation of a fully amorphous dispersion is crucial for the optimum enhancement of the dissolution rate of the poorly soluble drug^{3–6}. However, in contrast to usual expectation, a few reports have shown that the reverse is true whereby dispersion with some trace crystal do not decrease the so-called enhanced dissolution performances of solid dispersion system^{7–9}. The later reports have negated the theoretical concept of how an amorphous solid dispersion may contribute to the dissolution mechanism of a poorly soluble drug. Besides, the molecularly dispersed solid dispersion was suggested to be pertinent in increasing the surface area for the dissolution process. This theory was again negated by some

studies^{10,11}. For instance, a decrease in the release rate of itraconazole was noted in the solid dispersion of small (< 240 μm) and large (381–1400 μm) particle size fraction as compared to the intermediate size fraction (240–380 μm) which displayed the highest dissolution rate¹². According to the authors, this observation is attributed to the higher tendency of recrystallization of smaller particles as compared with the larger fraction sized particles¹³. Therefore, the use of product with small particle size may be compromised by the extensive precipitation and higher recrystallization tendency of the product^{4,10,12,13}.

Furthermore, insignificant changes of the dissolution profiles of SD after extreme storage condition such as 75% RH or high storage temperature (40 and 60 °C) have been reported^{7,14–19}. Bruce et al. reported similar dissolution profiles between the fresh SD and aged SD despite the growth of crystal on the surface of the aged tablet¹⁴. This may be due to the sigmoidal recrystallization profile for most of the amorphous drug which showed an accelerated recrystallization rate at early recrystallization process and subsequent slower growth of crystalline material in its sample. Slower crystal growth at the later stage of the crystallization profile may responsible for the lower recrystallization tendency upon dissolution process. In another study, Jijun et al. have demonstrated that a short period of high storage temperature or also known as “post heating” gave rise to a low solution mediated recrystallization

tendency and therefore it sustains the supersaturation state during dissolution¹⁵. However, the detail of the mechanism on how it yields this advantage from this “post heating” effect is still poorly understood.

When a fully amorphous dispersion is exposed to the aqueous environment, it creates supersaturation which is the driving force for extensive agglomeration and recrystallization in the hydrodynamics of dissolution vessel^{20,21}. In order to limit the extensive precipitation and high tendency of recrystallization, here we suggested that a post-processing treatment may be needed to get a physically stabilized solid dispersion. In light of this, the tendency of recrystallization during dissolution process is expected to decrease after the formulation has undergone the high rate of early recrystallization process before the dissolution procedure. Moreover, the recrystallized drug, which is known to have lower molecular mobility, is expected to have a lower degree of agglomeration. Hypothetically, this will lead to a theoretically stabilized and dissolution enhanced solid dispersion.

Therefore, this study tested the effect of a post-processing treatment on the dissolution performance of a SD in comparison to their performance upon production. Two poorly soluble drugs were used in this investigation i.e. ketoprofen (KTP) and piroxicam (PIX). KTP and PIX are Non-steroidal anti-inflammatory drugs (NSAID) that belong to Biopharmaceutical Classification System (BCS) Class II drugs^{8,22}. Polyvinyl alcohol (PVA) is chosen as a carrier in order to produce a crystalline dispersion and compare the essentiality of obtaining a fully amorphous dispersion for the enhanced dissolution performance as reported in the previous studies. Both model drugs were formulated into crystalline solid dispersion by utilizing spray-drying method. After the spray dry production, the obtained samples were post processing treated by exposure to high humidity condition, i.e. 75% RH at room temperature. Dissolution performances of the post processing treated samples were then compared to the freshly prepared samples in relation to their physical states.

Materials and methods

Materials

KTP was purchased from AFINE Chemical LTD, BN: 1102017, whereas PIX was obtained from Novaltek Lifescience, Shanghai (PR China). The hydrophilic polymer PVA was obtained from BDH Laboratory, England.

Preparation of physical mixture and spray-dried solid dispersion

Various compositions of solid dispersion KTP-PVA and PIX-PVA systems were prepared (Table 1). A total of 5.0 g of the model drug and PVA according to the proportions were completely dissolved using 50% v/v ethanol in water. The solution were then spray-dried using a Buchi mini-spray dryer B-290 (BÜCHI Labortechnik AG, Switzerland) with parameter shown in Table 1. On the other hand, physical mixture (PM) of drugs and polymers based on the corresponded drug content of the SD (Table 1) were prepared by gentle

mixing of the weighed powders using a mortar and pestle. Melt-cooled of the pure drugs were also prepared for comparison purpose. The pure crystalline drugs were melted on top of hot plate at 10 °C above melting temperature of the drugs. After the drugs were fully melted, it was allowed to isotherm for 5 min. The melted drugs were then cooled at room temperature to produce amorphous solid.

Characterization of the spray-dried KTP-polymer solid dispersions

Solid state characterization of the prepared SD and PM of KTP-PVA and PIX-PVA was carried out by Differential Scanning Calorimetry (DSC), Attenuated total reflectance- Fourier transform infrared (ATR -FTIR) and X-ray powder diffraction (XRPD).

Water content measurement

Water content of the obtained samples was determined by heating ~10 mg of sample using a hotplate at 100 °C for 10 min. The weight of the samples before and after heating was recorded. The percentage of weight loss after 10 min of heating at 100 °C was taken as the function of water content in the sample.

DSC measurement

DSC measurements were performed with PerkinElmer Pyris 6 DSC (PerkinElmer, Singapore). The weight of circa ~2–4 mg of samples was packed in crimped aluminum pan and heated under dry nitrogen purge. Samples were heated from 0 °C to 220 °C and 0 °C to 250 °C at 10 °C/min for KTP and PIX, respectively to cover the thermal characteristic of both model drugs. The obtained results were analyzed using Pyris Data Analysis software (PerkinElmer, Singapore).

ATR-FTIR spectroscopy

ATR-FTIR spectra were recorded over a wavenumber range of 500–4000 cm⁻¹ with a resolution of 4 cm⁻¹ and 32 scans using Thermo Nicolet FTIR Nexus spectrometer (Thermo Electron Corporation, Waltham, MA) coupled with ATR accessory. The spectra were analyzed using OMNIC software (Thermo Electron Corporation, Waltham, MA).

XRPD analysis

XRPD analysis of raw materials, PMs and SD were performed with a XRD, Bruker D8 Advance equipped with a copper X-ray Tube (1.54060 Å). Samples were pressed into a sample holder to generate a flat and smooth plane surface. The samples were then exposed to an X-ray beam with voltage of 40 kV and a current 40 mA. All measurements were performed from 3° to 50° (2θ) coupled with scanning speed of 0.02°/step and 1 s for every scan step to cover the characteristic X-ray diffracted peaks of the crystalline KTP and PIX.

UV-vis spectroscopy

To quantify the API content in a medium sample, a PerkinElmer Lambda 25 UV-vis spectrophotometer (PerkinElmer, Singapore) was used. The wavelength λ_{\max} specified for KTP which was identified to be devoid of any interference from the added carrier at 259 nm was used. Calibration curves were constructed for known concentration of KTP in distilled water at 259 nm by using Beer Lambert plots. Each point in the calibration line was an average

Table 1. Solid dispersion formulations prepared using spray drying method.

Systems	Drug content (%wt)	Processing parameters
KTP-PVA	30%	Inlet temperature 80 °C; outlet temperature 60 °C; feeding pump rate of 5%; aspirator of 80%
	50%	
PIX-PVA	10%	Inlet temperature 110 °C; outlet temperature 84 °C; feeding pump rate of 5%; aspirator of 80%
	30%	

value of three measurements. The same procedure was carried out for PIX at wavelength λ_{\max} of 360 nm.

Dissolution and intrinsic dissolution studies

Dissolution tests were performed using paddle method in a calibrated Varian VK7000 Dissolution Apparatus (Varian, Inc. Weston Parkway Cary, NC). A total of 900 mL of distilled water was used as a dissolution medium. The dissolution medium was set at $37.0 \pm 0.5^\circ\text{C}$ and the paddle speed of 50 rpm was used. Pure drug, polymer, PM and SD products which were sieved to a controlled particle size range of 100–106 μm were added to the dissolution medium upon the start of dissolution experiment. Then 10 ml of the samples was withdrawn at 2, 5, 10, 15, 20, 30, 40, 50, 60 and 120 min (up to 180 min for PIX-PVA system). The volume of dissolution medium withdrawn was immediately replaced by introducing the same volume of fresh medium into the dissolution vessel. The samples were then filtered with mixed cellulose ester microfilter of 0.45 μm pore size (MFS membrane filter, Lot no. 41CLCA) and analyzed for content of KTP and PIX using UV-vis spectroscopy at 259 and 360 nm, respectively. The release studies were carried out in sink condition for SD KTP-PVA systems and non-sink for SD PIX-PVA systems due to the extremely low solubility of PIX.

To compare the dissolution performances among the investigated systems, dissolution efficiency was calculated using the trapezoidal method which was expressed as a percentage of the area of rectangle divided by the area of 100% dissolution in the same time as shown in Equation (1)^{23,24}.

$$DE (\%) = \frac{\int_0^t y dt}{y_{100} t} \times 100\% \quad (1)$$

Intrinsic dissolution studies were performed using stationary disc method²⁵. Powder samples were compressed for 1 min into a stainless steel cylinder with the formation of disc at one side of the cylinder with diameter of 8 mm (surface area of 0.5027 cm^2) using a laboratory hydraulic press (Kimaya Engineers, Thane West, Maharashtra, India). The holder with compact powder were placed

in the dissolution vessel filled with distilled water set at $37 \pm 0.5^\circ\text{C}$ as dissolution medium. In the stationary disc method, paddle was rotated at 50 rpm at a position one inch on top of the stationary disc which was exposed to the medium. Medium samples were withdrawn at predetermined time namely, 2, 5, 10, 15, 20, 25, 30 min up to 1 h. The collected samples were analyzed at their corresponding UV wavelengths as described in previous paragraph.

Deliberate post-processing treatment of the freshly prepared solid dispersion

Saturated solution of sodium chloride (NaCl) was used to create the 75% RH condition in a desiccator. The freshly prepared SD was deliberately post processing treated in the $75 \pm 5\%$ RH at room temperature. The samples were placed in a sample tube without capping and exposed to the high humidity condition in a grease-sealed desiccator. The post processing treated SD products were then taken for physical characterization and dissolution studies as stated in the previous paragraphs.

Results

Water content

Figure 1 shows water content of all systems. Spray dried products have the lower water content in comparison to the PM. The low moisture content of SD products was due to the water evaporation from mixture during spray drying condition. The presence of high water content in SD 30 PIX-PVA indicates that the product is not completely dried after spray drying. As expected, water content of treated SD products increases after storage in a humid condition for 7 days.

Infrared radiation spectra analysis

ATR-FTIR spectrum of crystalline KTP shows a triplet at the region of 704 cm^{-1} (Figure 2). However, when KTP was converted into

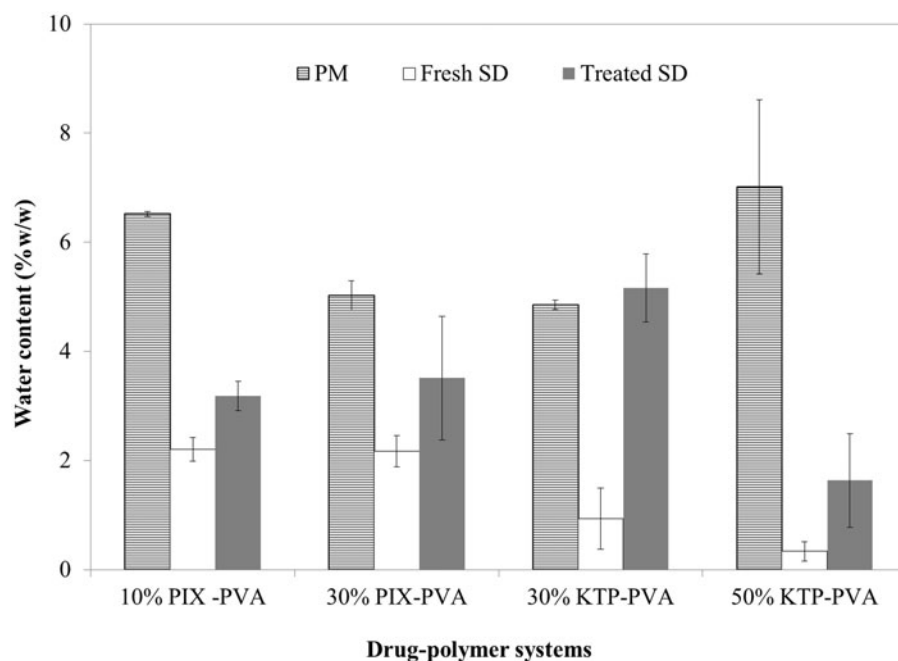


Figure 1. Water contents of PM, fresh SD and treated SD (7 d in 75%RH) of KTP-PVA and PIX-PVA.

amorphous (using melt-cooled method⁸), a doublet peak at the region of 704cm^{-1} and a shoulder at 1737cm^{-1} were revealed (Figure 2(c)). This may be corresponding to the breaking of the hydrogen bond involving carbonyl group of the KTP. Therefore,

the shoulder at 1737cm^{-1} and doublet at fingerprint region between 716 and 690cm^{-1} may be used as indication of amorphicity of the KTP. Looking at the spectra of SD, triplet peaks at 704cm^{-1} and the shoulder at 1737cm^{-1} were seen in both 30 and

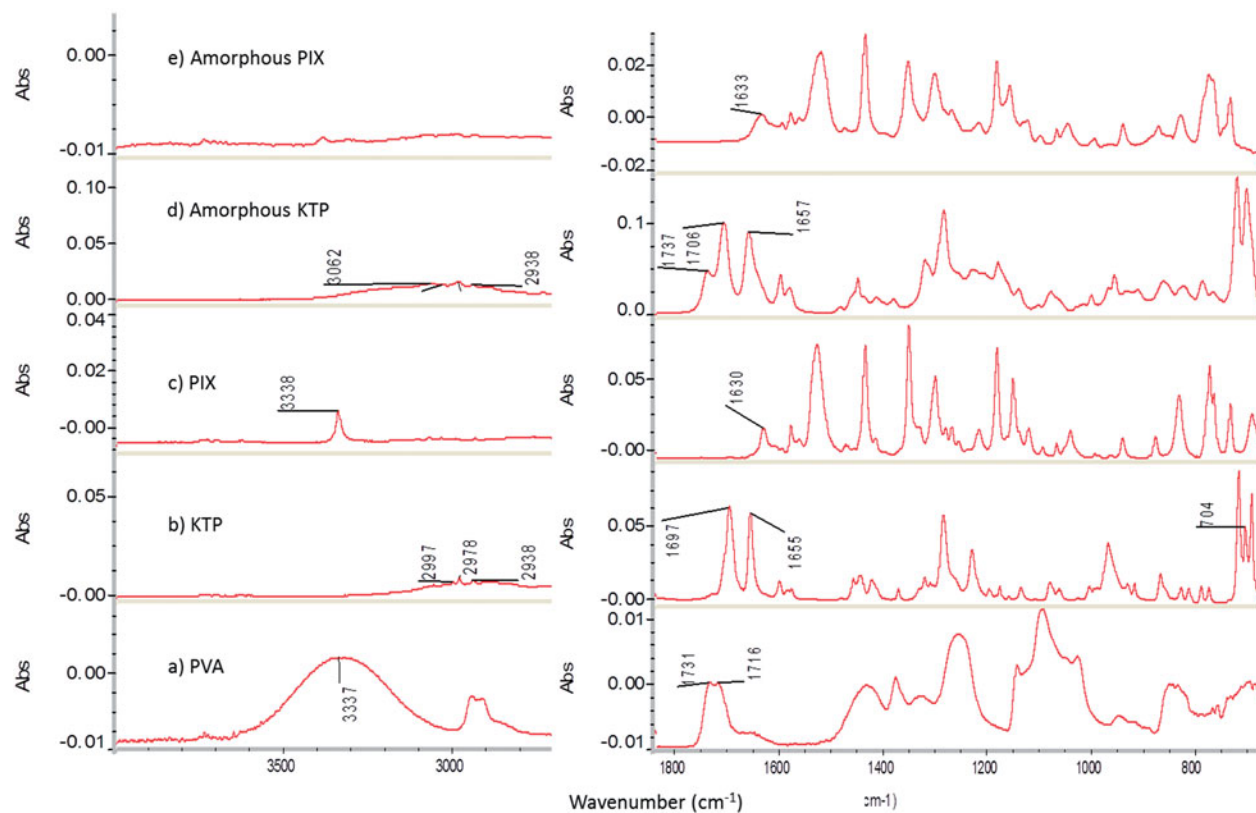


Figure 2. ATR-FTIR spectra of PVA, crystalline KTP, crystalline PIX, amorphous KTP and amorphous PIX.

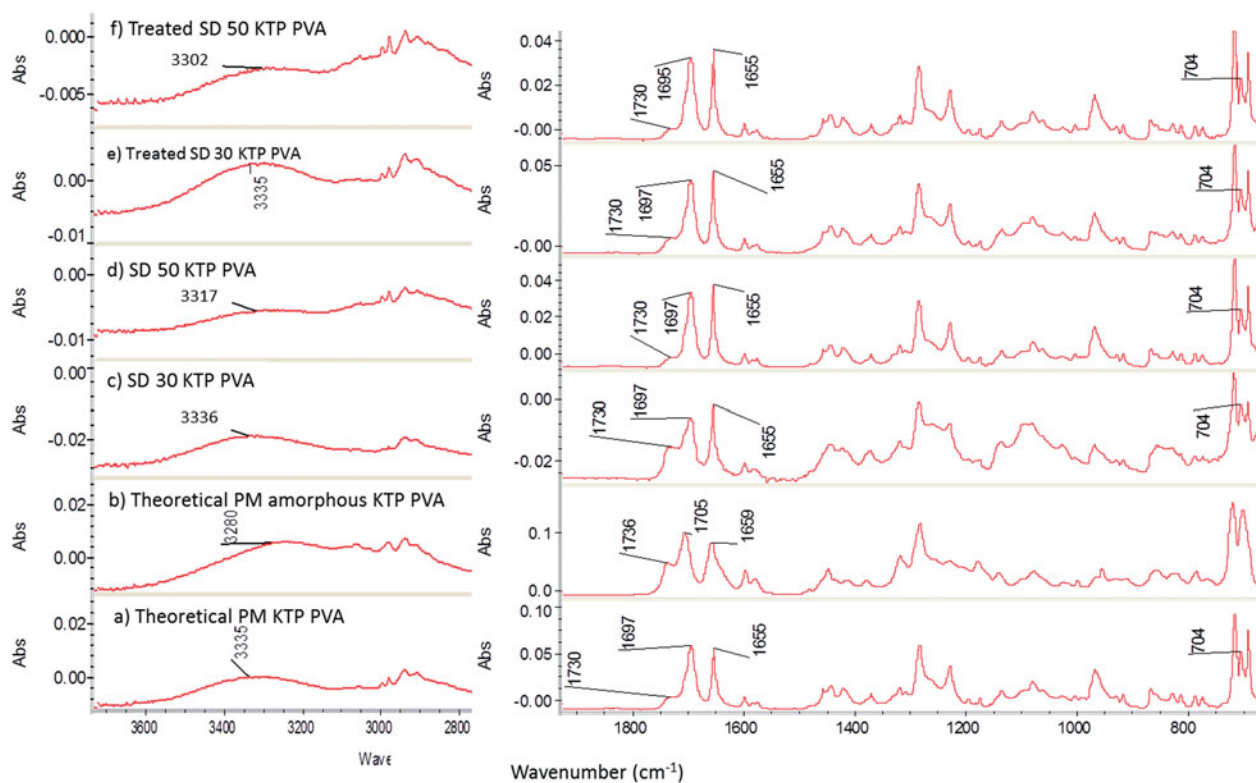


Figure 3. ATR-FTIR spectra of theoretical PM KTP-PVA, the corresponding fresh SD systems and treated KTP-PVA SD systems in 75% RH for one week.

50 KTP-PVA which suggests the present of crystalline material in these formulations (Figure 3(c) and (d)).

Besides, spectrum of the treated SD 30 KTP-PVA shows a reduction in intensity of the shoulder band at 1737 cm^{-1} (compare Figure 3(c) and (e)) which suggests an increase in crystallinity after storage in 75% RH. This may possibly due to the massive amount of water absorption that was indicated by the broad OH stretching at 3336 cm^{-1} which increases molecule mobility and hence promote recrystallization.

ATR-FTIR spectrum of crystalline PIX indicates a main peak at region of 3338 cm^{-1} which corresponds to the O-H stretching of alcohol group (Figure 2(c)). A new emerging peak at circa 3392 cm^{-1} was seen in both fresh SD of 10 and 30 PIX-PVA (Figure 4(c) and (d)). This indicated the presence of Form II PIX in the samples²⁶.

After one week humidity treated of SD PIX-PVA, intensity of crystalline peaks at 3338 and 3393 cm^{-1} was increased (Figure 4(e) and (f)). This indicates that recrystallization has taken place during the exposure to high humidity condition. In the IR spectra of the humidity treated SD 30 PIX PVA, the intensity of the peak at 3394 cm^{-1} , which corresponds to Form II PIX, was noted to be higher than that of 3338 cm^{-1} . This suggests that the SD system recrystallized preferably into Form II instead of the initially used polymorph, Form I.

Table 2 displays wavenumbers for selected characteristic bands for both the KTP-PVA and PIX-PVA systems. In order to conclude drug-polymer interaction, there shall be band down shifting of functional groups on both the drug as well as polymer. Based on Table 2, the functional band of OH from PVA at 3337 cm^{-1} showed almost no shifting/insignificant shift in the freshly prepared SD, therefore we could not conclude the existence of drug-polymer interaction.

DSC analysis

As a reference, DSC thermogram of pure APIs and PVA were shown in Figure 5. Based on Figure 5, melting temperature of KTP and PIX were detected at 96.31 and 202.68°C , respectively. PM of the KTP-PVA reveals a melting endotherm at circa 96°C which corresponds to the melting temperature of KTP (Figure 6(a) and (b)). Melting point of KTP was depressed to circa 86.37°C in the fresh SD 30 KTP-PVA (Figure 6(c)). This depression suggests the changes in chemical potential of KTP with the presence of PVA after spray drying process^{8,27}. Besides, the enthalpy changes was also reduced to 1.39 J/g which suggests the presence of a much smaller portion of crystalline KTP in the SD systems in comparison to the PM system. Similar deduction can be seen in the fresh SD 50 KTP-PVA (Figure 6(d)).

After humidity storage, the treated SD 30 KTP-PVA reveals a much higher value of enthalpy, $\Delta H = 18.6\text{ J/g}$ (Figure 6(e)). This indicated the higher amount of crystalline material in the treated SD 30 KTP-PVA system which suggests that recrystallization has taken place during the post-processing treatment. Limited changes were observed in enthalpy of treated SD 50 KTP-PVA systems after one-week exposure in 75% RH (Figure 6(f)).

The absence of melting peak in SD 10 PIX-PVA (Figure 7(c)) indicates the absence of detected crystalline PIX. This result is in contrast to the result of IR as Form I PIX was detected at 3392 cm^{-1} . This may be attributed to the dissolution of the crystalline trace of PIX into the polymer upon heating scan in DSC⁸. Similarly, there was no detected melting peak in the treated SD 10 PIX-PVA (Figure 7(e)) possibly due to the same reason quoted for the fresh SD 10 PIX-PVA system.

Conversely, a tiny melting endotherm at 195.62°C was detected in DSC thermogram of SD 30 PIX-PVA. Besides, the shape of the

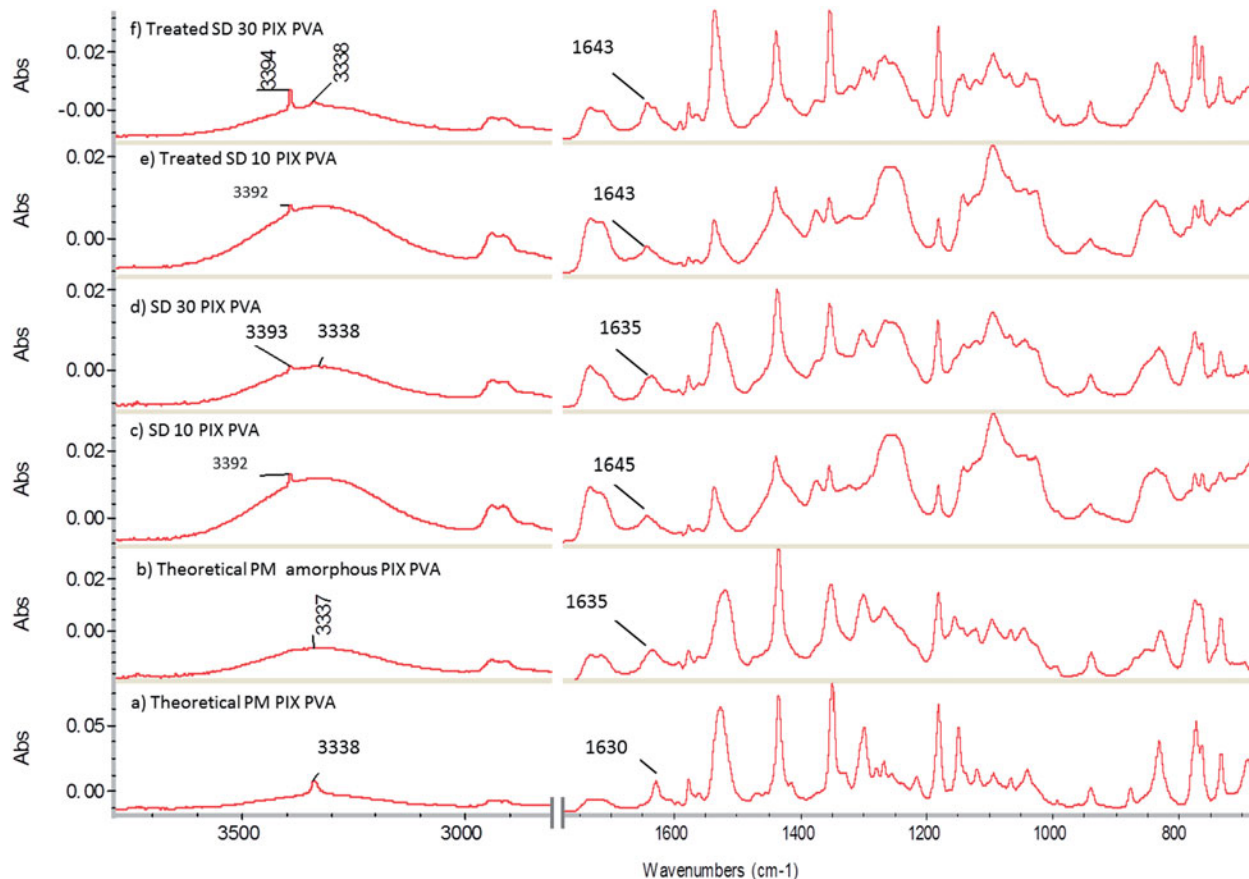


Figure 4. ATR-FTIR spectra of theoretical PM PIX PVA, the corresponding fresh SD and treated PIX-PVA SD systems in 75% RH for one week.

Table 2. Wavenumbers for selected characteristic bands of the investigated systems.

System	Selected wavenumber (cm ⁻¹)	Group contribution	Theoretical PM	SD	Treated SD
30 KTP-PVA	704	Crystalline KTP	Present	Present, lower intensity than pure drug	Present, lower intensity than pure drug
	1600–1700	C = O	Present	Present, no shifting	Present, no shifting
	1730	C = O of amorphous KTP	Absent	Present	Present
	2800–3000	CH ₂ stretching	Present	Broaden	Sharpen after treatment
	3337	OH	Present	Present, no shifting	Present, no shifting
50 KTP-PVA	704	Crystalline KTP	Present	Present, lower intensity than pure drug	Present, lower intensity than pure drug
	1600–1700	C = O	Present	Present, no shifting	Present, no shifting
	1730	C = O of amorphous KTP	Absent	Present	present
	2800–3000	CH ₂ stretching	Present	Broaden	Sharpen after treatment
	3337	OH	Present	Present, no shifting	Present, no shifting
10 PIX-PVA	3338	OH stretching	Present	Absent	Absent
	3392–3394	OH stretching of polymorph II	Absent	Present	Present
30 PIX-PVA	3338	OH	Present	present	Present with a slight increment in intensity compared to fresh SD
	3392–3394	OH stretching of polymorph II	Absent	present	Present with a slight increment in intensity compared to fresh SD

The position shift of SD systems is compared to the spectra of pure compound.

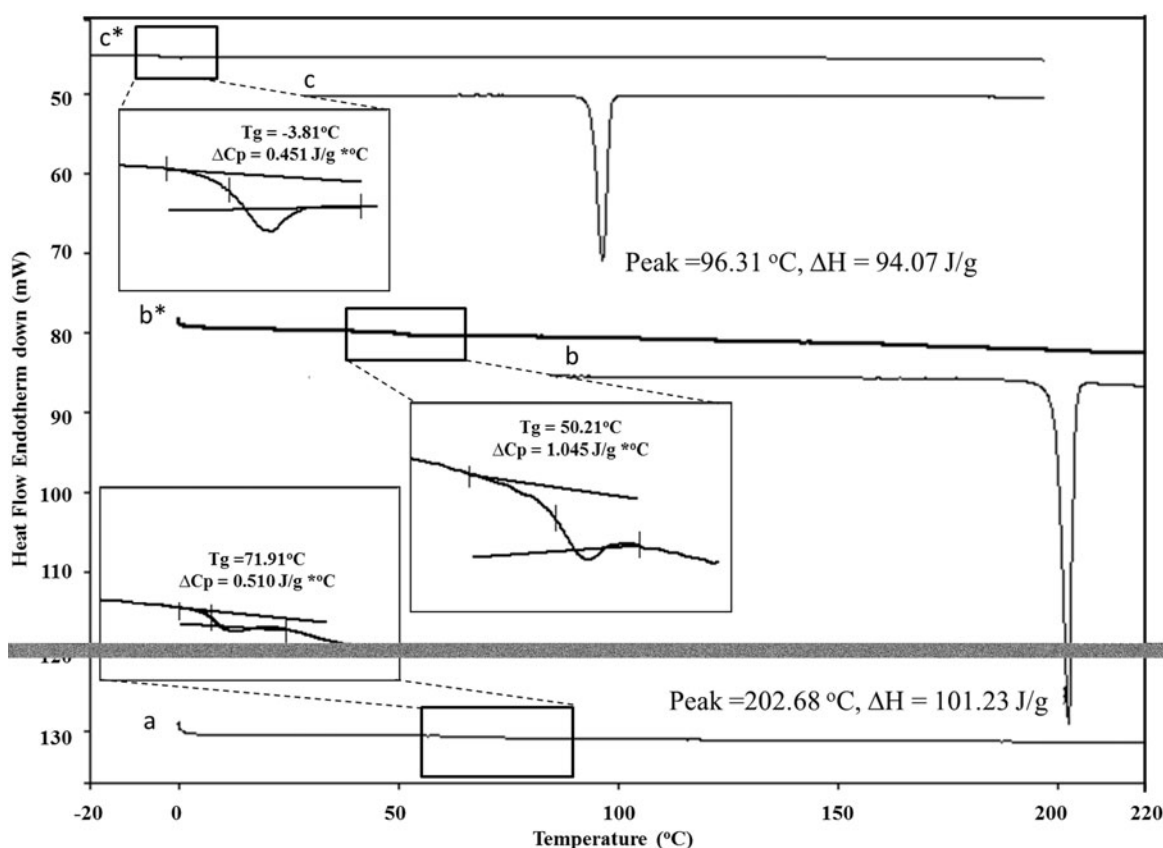


Figure 5. DSC thermograms of pure compounds, (a) PVA, (b) first heating of crystalline piroxicam, (b*) second heating of piroxicam, (c) first heating of crystalline etoprofen, (c*) second heating of ketoprofen.

endotherm was a summation of two endotherm peaks which is shown in the enlarged insert (Figure 7(d), boxed). This might be related to the melting of the two different forms of PIX. The doublet endotherm became more obvious in the thermogram of treated SD samples (Figure 7(f), boxed).

X-ray powder diffraction analysis

X-ray powder diffractograms of the KTP and PIX samples are shown in Figures 8 and 9, respectively. In KTP system, peaks intensities in region of 8–28° were reduced in the fresh SD 30 KTP-PVA system comparatively to their corresponding PM systems (Figure 8). After the post-processing treatment in 75% RH, intensities of the

crystalline peaks increased which suggested an increment in crystallinity of KTP (Figure 8(c) and (d)). However, only limited changes were seen in treated SD 50 KTP-PVA system after the post-processing treatment.

Form I PIX, which was used as initial material in this study, shows a typical diffracted peak at 8.62° (Figure 9). This peak was not observed in both the freshly SD 10 and 30 PIX-PVA but a shifted peak at 9.09° together with new emerging peaks at 15.60 and 25.51° were observed in the diffractograms of fresh SD 10 and 30 PIX-PVA systems. This indicates the presence of different polymorphs of PIX in these SDs. The new peaks noted were consistent to Form II PIX²⁶. After exposure in 75% RH, the intensities of these diffracted peaks were obviously increased (Figure 9(c) and (d)).

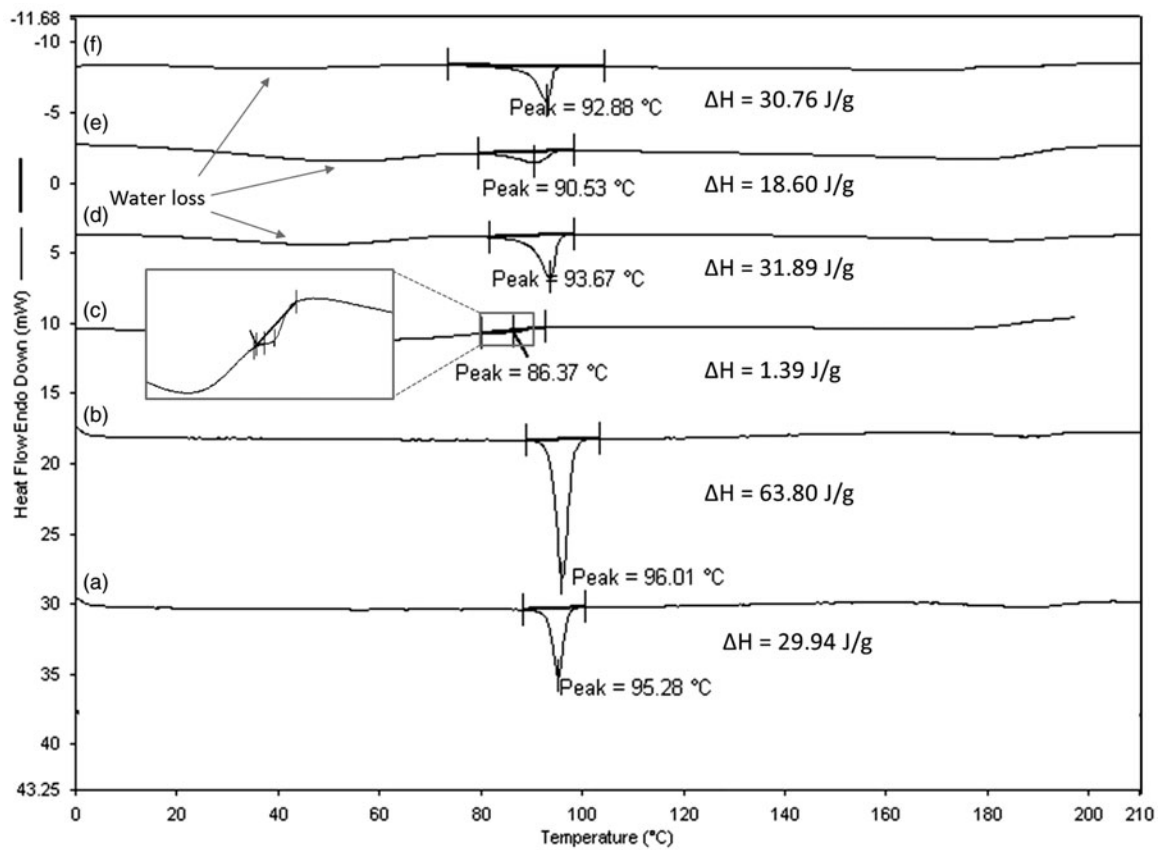


Figure 6. DSC thermograms of (a) PM 30 KTP-PVA, (b) PM 50 KTP-PVA, (c) fresh SD 30 KTP-PVA, (d) fresh SD 50 KTP-PVA, (e) treated SD 30 KTP-PVA and (f) treated SD 50 KTP-PVA.

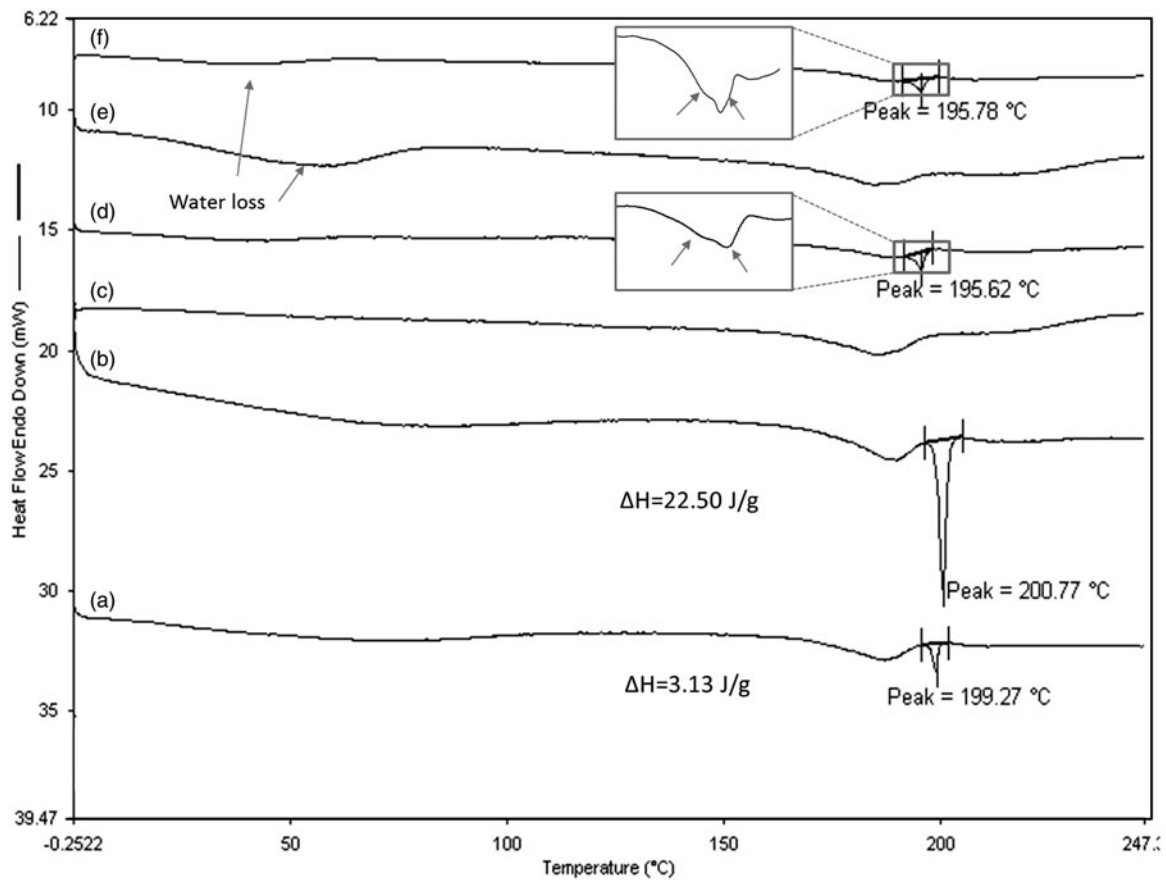


Figure 7. DSC thermograms of (a) PM 10 PIX-PVA, (b) PM 30 PIX-PVA, (c) fresh SD 10 PIX-PVA, (d) fresh SD 30 PIX-PVA, (e) treated SD 10 PIX-PVA, and (f) treated SD 30 PIX-PVA.

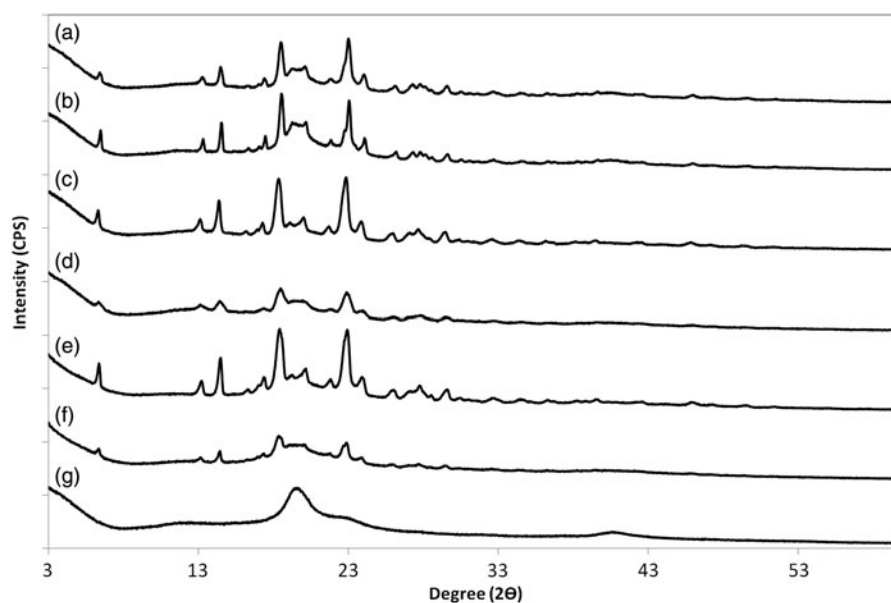


Figure 8. X-ray Diffractograms of the investigated samples, (a) PM 50 KTP-PVA, (b) PM 30 KTP-PVA, (c) treated SD 50 KTP-PVA, (d) treated SD 30 KTP-PVA, (e) fresh SD 50 KTP-PVA, (f) fresh SD 30 KTP-PVA and (g) PVA.

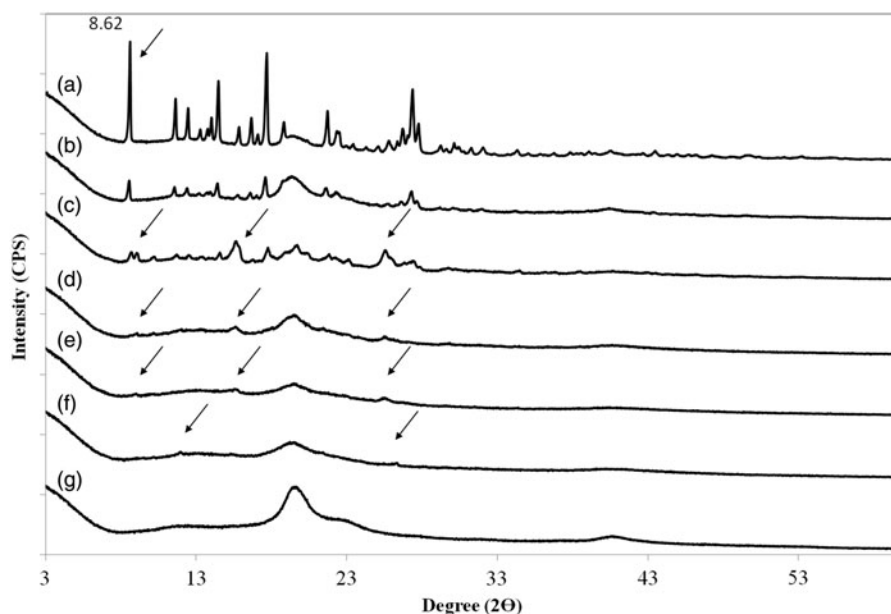


Figure 9. X-ray diffractograms of the investigated samples, (a) PM 30 PIX-PVA, (b) PM 10 KTP-PVA, (c) treated SD 30 PIX-PVA, (d) treated SD 10 PIX-PVA, (e) fresh SD 30 PIX-PVA, (f) fresh SD 10 PIX-PVA and (g) PVA.

Table 3. Crystallinity of the PM, fresh SD and treated SD samples based on integrated area of the X-ray diffractogram.

Formulations	Area under X-ray diffractogram	Crystallinity (%)
PM 30 KTP-PVA	13 835	30
PM 50 KTP-PVA	21 066	50
SD 30 KTP-PVA	6206	13.46
SD 50 KTP-PVA	20 793	49.35
1w 30 SD KTP-PVA	9065	19.66
1w 50 SD KTP-PVA	19 612	47.16
PM 10 PIX-PVA	7863	–
PM 30 PIX-PVA	24 905	–
SD 10 PIX-PVA	2158	–
SD 30 PIX-PVA	3730	–
1 week SD 10 PIX-PVA	2375	10.05 ^a
1 week SD 30 PIX-PVA	13 854	271.42 ^a

^aIn solid dispersion of PIX-PVA, a different polymorph, Form II, was detected. With that, the comparison of the SD to the PM in different form could not be made. Hence the crystallinity changes of the post processing treated SD PIX-PVA was calculated based on the initial integrated area of the peaks in freshly prepared SD.

Table 3 presents the crystallinity quantitated from the area under the integrated peaks of X-ray diffractogram using the PM as reference of 100% crystallinity. Crystallinity of the fresh SD 30 KTP-PVA systems was half of the PM. After the post-processing treatment, the treated SD 30 KTP-PVA revealed further increment in crystallinity, i.e. from 13.46 to 19.66%. The treated 50 KTP-PVA showed only limited crystallinity change which is in consistent to the result deduced from DSC and ATR-FTIR.

Similarly, crystallinity of the both the treated samples of SD 10 and 30 PIX-PVA have increased. The increments are about 10 and 271% for the treated SD 10 and 30 PIX-PVA, respectively.

Dissolution performances

Table 4 summarized the dissolution efficiency of the all the investigated systems (Equation 1). Dissolution rate of SD 30 KTP-PVA system was noted higher than its PM system. However, high

deviations of the initial release profile with obvious reduction in the release of KTP at later stage of the process were observed (Figure 10). Dissolution performance of post processing treated SD 30 KTP-PVA was not significantly reduced after the post-processing treatment. At 10 min, dissolution of the treated system overtakes the fresh SD. The slowed initial dissolution rate might be ascribed to the increased crystal material due to solution-mediated recrystallization that reduces the overall wetting of the system.

Unlike SD 30 KTP-PVA system, dissolution rate of SD 50 KTP-PVA was noted to increase even though the concluded crystallinity of this system is similar to that of PM (Figure 11). More interestingly, the system reveals a much faster initial dissolution rate after one-week exposure in 75% RH despite the similar crystallinity before and after treated. This result is intriguing that there might be a subtle process occurring during the storage in extreme condition which leads to the faster dissolution rate of the treated samples.

As expected, dissolution of the fresh SD 10 PIX-PVA shows a dramatic increase in initial dissolution rate of PIX in the fresh SD system due to the high percentage of conversion from crystal material to its corresponding amorphous form after spray drying (Figure 12). A similar trend was also seen in 30 PIX-PVA system whereby the fresh SD show increased dissolution rate and further increase in the release rate was seen in the post processing treated sample (Figure 13). This is unexpected as the increased in crystallinity of PIX in the treated SD 30 PIX-PVA shall theoretically deteriorate the overall release rate. In order to clarify the unexpected results, which may possibly be attributed by the fluffiness of the fresh sample that float on top of dissolution medium, intrinsic dissolution rate of all the samples (IDR) were examined.

Table 4. Dissolution efficiency of the investigated systems after 120 min of dissolution process.

Systems	DE ₁₂₀ ±standard deviation (%)			
	Pure drug	PM	SD	Treated SD
30 KTP-PVA	76.72 ± 3.14	58.00 ± 3.05	92.15 ± 1.58	97.69 ± 0.18
50 KTP-PVA	76.72 ± 3.14	81.99 ± 12.61	94.27 ± 1.67	96.07 ± 1.45
10 PIX-PVA	28.61 ± 4.33	31.66 ± 2.82	72.66 ± 14.35	87.02 ± 1.91
30 PIX-PVA	28.61 ± 4.33	30.92 ± 5.06	79.40 ± 1.00	89.79 ± 0.47

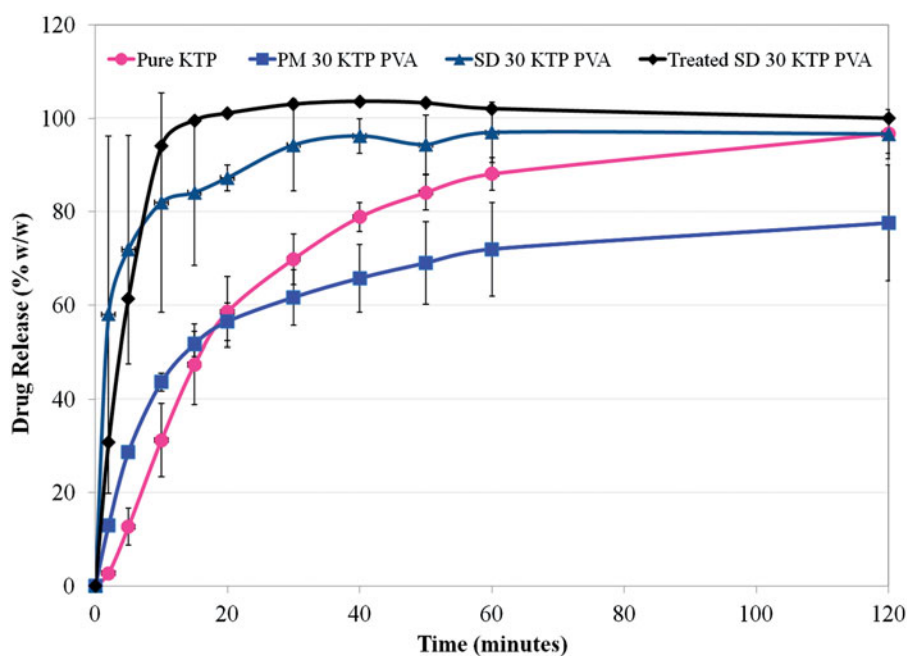


Figure 10. Dissolution profiles of pure KTP, PM, fresh SD and treated SD of 30% KTP-PVA.

Based on the IDR tests, it is worth mentioning that there was an initial surge of drug release detected in most of the investigated systems (Figures 14 and 15). The initial surge was then followed by a dramatic drop of drug concentration, a profile that usually seen for dissolution of a supersaturation system indicating recrystallization²⁸. The IDR values of these systems were calculated based on the linear drug release of the systems after the event of initial surge release (Table 5). Looking into the initial surge phenomenon, the fresh samples tend to show a higher surge than the treated samples particularly in SD KTP-PVA systems (Figure 14). This surge has also been noted in all the SD PIX PVA systems but to a lesser extent (Figure 15). In parallel to the dissolution studies, IDR of most of the treated samples were consistently higher than their corresponding fresh systems. This parameter could be clearly presented by the IDR ratio of the SD system to pure drug (Table 5) whereby IDRs have increased from 2 folds to 3 folds and 2 folds to 11 folds for both treated SD of 10 and 30 PIX-PVA systems, respectively. Similarly, the same trend was observed in treated SD 50 KTP-PVA system. With exception, treated SD 30 KTP-PVA system did not show a higher IDR rate but rather it shows a lower average of IDR with the standard deviation overlapped to the IDR of the fresh sample. Furthermore, the result is in line to the observed dissolution curve where treated 30 KTP-PVA system reveals an almost similar or slower release rate at initial stage of KTP release (Figure 10). This implies the insignificant different between IDR of treated and fresh SD 30 KTP-PVA system. Overall the IDR results suggested that the improvement of dissolution behavior of the post processing solid dispersion is related to their inherent characteristics rather than the buoyancy of the fresh particles in the convection of medium while dissolution experiment.

One of the inherent characteristics of the SD would be apparent solubility of the generated systems. This parameter was examined to confirm its contribution to the observed anomalous dissolution trend. SD KTP-PVA showed at least one fold increment in solubility for all the tested fresh and treated SD systems (Table 5). Solubility of PIX has increased at least three folds in fresh SD system and almost five folds in the treated SD PIX system. Interestingly, apparent solubility of all the treated solid dispersion systems consistently

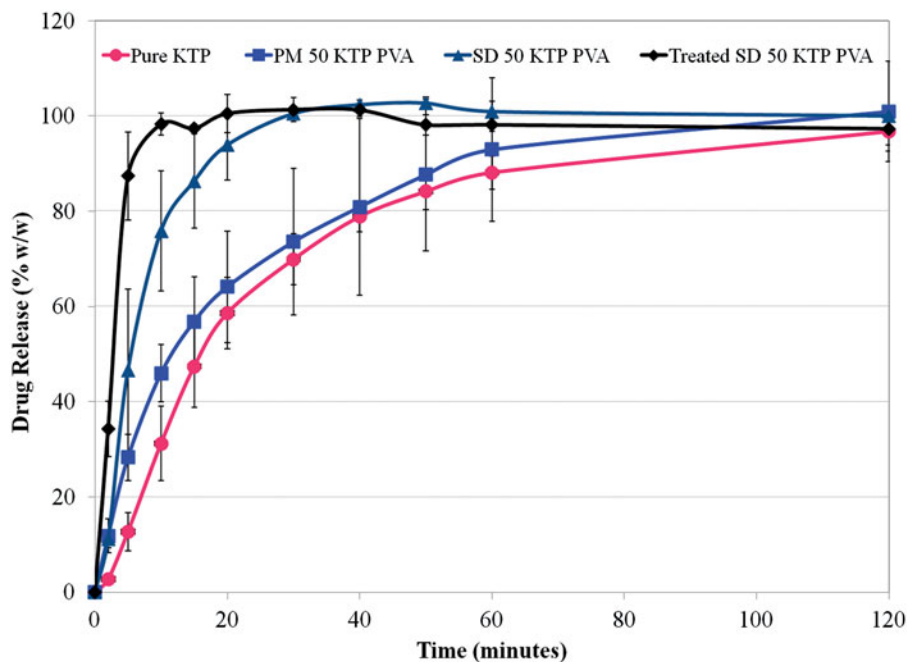


Figure 11. Dissolution profiles of pure KTP, PM, fresh SD and treated SD of 50% KTP-PVA.

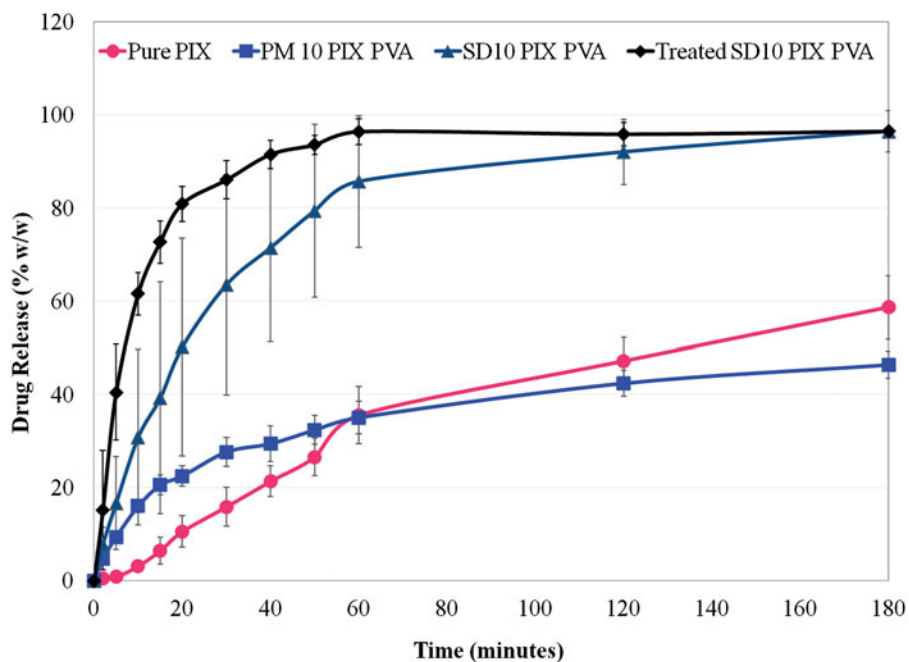


Figure 12. Dissolution profiles of pure PIX, PM, fresh SD and treated SD of 10% PIX-PVA.

showed higher solubility values in comparison to the fresh SD system after 24 h stirring at room temperature. The IDR tests have further supported the anomalous trend seen in dissolution performances of the treated SD system.

Discussion

Water is a well-known plasticizer which may promote recrystallization of the product, particularly the humidity-stored products. From the presented result, the post processing treated SD in high humidity condition revealed higher moisture content due to the massive water absorption during the humidity exposure. This has subsequently promoted the recrystallization of the product which can be evidenced by the typical crystalline bonding and melting

temperature detected in both the ATR-FTIR and DSC measurement. In addition, the partially amorphous systems of the fresh and post processing treated SD were further confirmed using XRPD method.

As expected, partial amorphicity of the freshly prepared SD system has contributed to the enhanced dissolution rate of the fresh SD system as compared to its corresponding PM system. This may be due to dissolution enhancement through high energy of amorphous state, hydrophilicity of carrier system, formation of soluble complexes, increase surface area etc.^{4,29}. Theoretically, the increment of crystallinity in a solid dispersion system will negate the dissolution performances of the formulation due to the lower solubility of the crystalline material as compared to the amorphous state^{5,30}. However, a reverse phenomenon was noted in this study. Despite the higher crystallinity that was quantitated in the post

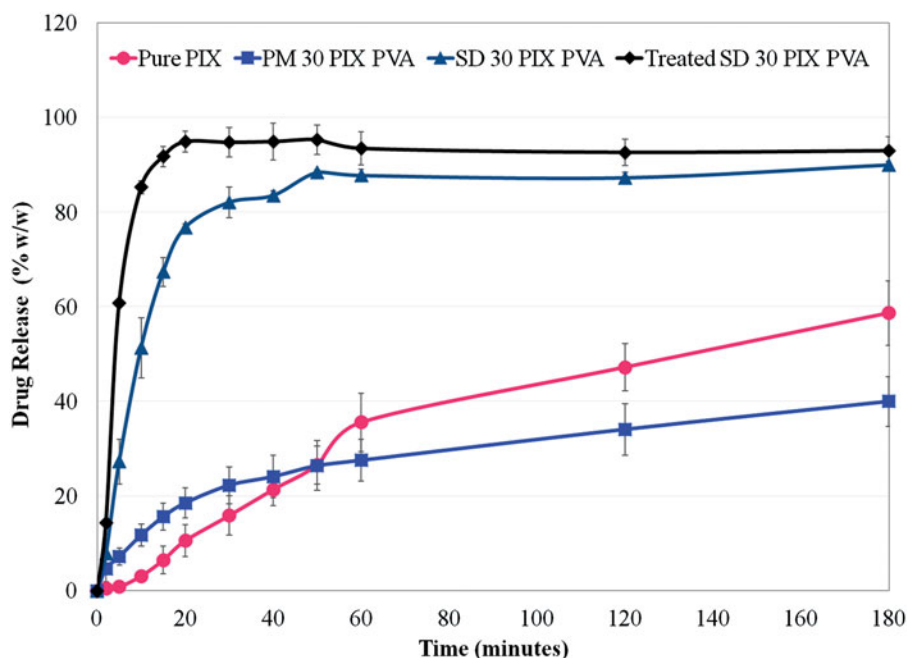


Figure 13. Dissolution profiles of pure PIX, PM, fresh SD and treated SD of 30% PIX-PVA.

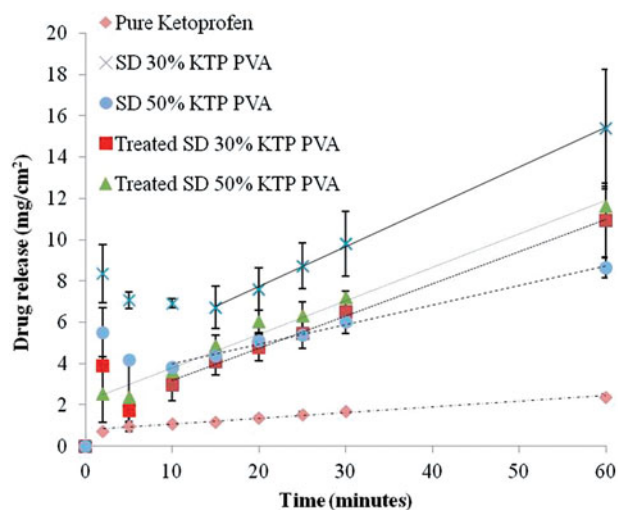


Figure 14. Intrinsic dissolution profiles of pure KTP, PM, fresh SD, treated SD of 30% KTP-PVA and 50% KTP-PVA.

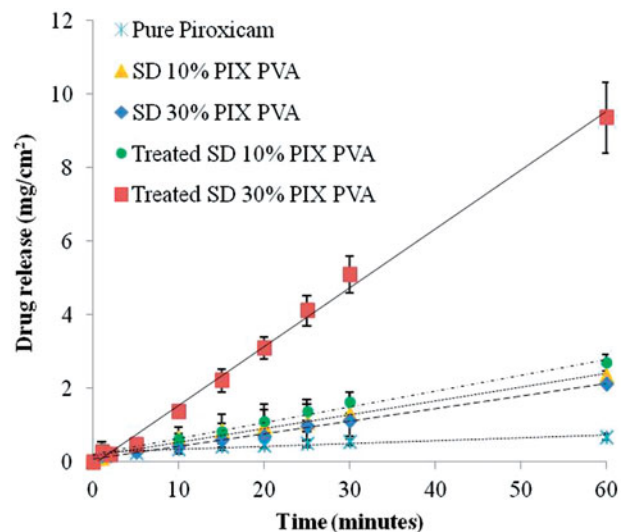


Figure 15. Intrinsic dissolution profiles of pure PIX, PM, fresh SD, treated SD of 10% PIX-PVA and SD 30% PIX-PVA.

processing treated SD systems, dissolution rate of the post processing treated samples were surprisingly and consistently faster with smaller deviation in comparison to the fresh one.

Similar observations were reported before with limited emphasis. For instance, the release rate of diazepam from SD PEG-diazepam after humidity storage (75% RH) was found to be higher than the corresponding sample desiccated at 0% RH³¹. Likewise, Gupta et al. reported an increase in dissolution rate of naproxen after storage¹⁶. In this study, the higher dissolution rate noted after the post processing humidity treatment suggested that dissolution rate of the fresh samples upon production was actually compromised. Confounding factor that contributed to the compromised dissolution rate of the fresh sample may be related to their extensive agglomeration during dissolution process which was consistent to the work presented recently⁸. As both the SD of 10 and 30 PIX-PVA showed the preferences in recrystallize conversion to Form II PIX, thus, the fact that ratio of Form I and Form II PIX may contribute to this unexpected dissolution profile could not be

excluded. Nevertheless, the increment in crystallinity after post-processing treatment and yet lead to the enhanced dissolution rate is an unexpected phenomenon which shall not be overlooked.

Amorphous is often related to high molecular mobility. As a result, when the particles with high molecular mobility are introduced into the dissolution medium, extensive agglomeration or solution mediated recrystallization of the drug is ripening^{4,32}. This effect could be seen through the dramatic reduction of drug concentration after initial surge of the IDR profile of the freshly prepared sample. The level of drug concentration reduction after the initial surge profile implies the tendency of recrystallization/agglomeration which was apparent in freshly prepared SD system. Instead of generating an improved dissolution system, this tendency may exacerbate the process of recrystallization and leads to extensive agglomeration or precipitation which eventually offset the benefit of "amorphous advantage" that we have thought thus far. Then, the drug and carrier may release as single entity which

Table 5. Solubility and intrinsic dissolution rate (IDR) of the freshly prepared solid dispersion (SD) system and post processing treated systems (treated under exposure in 75% RH for one week).

Formulations	IDR (mgcm ⁻² min ⁻¹)	R ²	IDR ratio SD/pure drug	Equilibrium/apparent solubility (mg/ml)
SD 10% PIX-PVA	0.0368 ± 0.0015	0.9983	2.67	0.0343 ± 0.00005
Treated SD 10% PIX-PVA	0.0426 ± 0.0132	0.9983	3.09	0.0614 ± 0.0003
SD 30% PIX-PVA	0.0341 ± 0.0005	0.9977	2.47	0.0308 ± 0.0008
Treated SD 30% PIX-PVA	0.1601 ± 0.0164	0.9977	11.16	0.0389 ± 0.0004
SD 30% KTP-PVA	0.1933 ± 0.0514	0.9945	7.05	0.2371 ± 0.0356
Treated SD 30% KTP-PVA	0.1564 ± 0.0288	0.9970	5.71	0.2624 ± 0.0364
SD 50% KTP-PVA	0.0950 ± 0.0214	0.9936	3.47	0.2351 ± 0.0336
Treated SD 50% KTP-PVA	0.1603 ± 0.0116	0.9962	5.85	0.2760 ± 0.0390
PIX	0.0138 ± 0.0008	0.9886	–	0.0107 ± 0.0001
KTP	0.0274 ± 0.0024	0.9842	–	0.1480 ± 0.0052

Generally, there is no significant structural change of the prepared IDR sample before and after compression which have been confirmed by comparing the X-ray diffractograms of the compressed and non-compressed samples (Refer to the supplementary data). The calculated area under XRPD peaks showed only a slight crystallinity different, i.e. less than 3.8% crystallinity different between the compressed and non-compress samples.

give rise to a slower release of drug at later stage³³. This has contributed the inconsistency of the dissolution performances of fresh SD system. Unlike the fresh sample, the post processing treated samples were exposed to a high humidity condition and allowed for early recrystallization and “annealing” at room temperature to relieve internal stress. Upon introducing into dissolution medium, the post processing treated samples were relatively stable with lower tendency of recrystallization (as it has been recrystallized in its solid state during humidity exposure). The lower recrystallization tendency would escape the exacerbation of further recrystallization and agglomeration during the dynamic convection of dissolution medium. Therefore, in this study, more predictable SD systems with partial amorphicity in its formulation are obtained after post-processing treatment as indicated by the smaller error bars of the repeated dissolution profiles in comparison to the freshly prepared SD systems.

Another factor that may have contributed to the increased in dissolution performances after humidity treatment is the increased of apparent solubility of the treated system. It is somewhat unexpected that apparent solubility of the treated systems was higher than the freshly prepared samples. The different solubility results between the fresh and treated sample indicated that the solubility is not purely related to the solubilizing capacity of the polymer but rather it is related to the solid modification of the treated system before the dissolution test³³. It has been reported that surface of the spray dry particles have comparatively lower wettability due to the adsorption of less soluble compound (more hydrophobic) at its liquid/air interface during the drying process³⁴. This may lead to extensive agglomeration via hydrophobic forces of the fresh sample upon contact in water based on the theory of Ostwald ripening. As the solubility tests in this study were performed for 24 h, it might not be enough for the fresh samples (which undergo extensive agglomeration) to achieve its equilibrium solubility. Unlike the fresh samples, the treated samples have undergone exposure in the humidity condition which may improve its wettability through the migration of its hydrophilic carrier to the surface of the particles. Hence, besides the reduced tendency of recrystallization/agglomeration, changes of the apparent solubility after post processing humidity treatment has partly contributed to the enhanced dissolution performance of treated samples.

Conclusion

This study highlighted the production of SD with enhanced dissolution performance after a post-processing treatment. Instead of generating an undesirable product with poor performances, a more stabilized system with a preferable enhanced dissolution rate was obtained by the short period (one week) post-processing

treatment in a high humidity condition. It is noted that the recrystallized traces after the post-processing treatment did not affect the dissolution profile of SD. Therefore, drug in SD need not necessarily exist in the fully amorphous state. Rather, partial amorphicity is adequate to enhance the dissolution performances. A fraction of the drug could be molecularly dispersed and other could be remained in crystalline state in the matrix, thus forming a dissolution-stabilized SD. Besides, solubility changes have been detected in humidity treated sample which could be a potential cause of their enhanced dissolution rates. More investigations should be carried out in order to unfold the mechanism behind the solid modification that increased apparent solubility of the humidity treated sample.

Disclosure statement

The authors report no declarations of interest.

Funding information

This work was supported by the short-term grant 304/PFARMASI/6313055 received from Universiti Sains Malaysia.

References

- Huang Y, Dai W-G. Fundamental aspects of solid dispersion technology for poorly soluble drugs. *Acta Pharm Sin B* 2014; 4:18–25.
- Lima ÁND, Santos PBS, Lyra MMD, et al. Solid dispersion systems for increase solubility: cases with hydrophilic polymers in poorly water soluble drugs. *Braz J Pharmacy* 2011; 4:269–78.
- Langham ZA, Booth J, Hughes LP, et al. Mechanistic insights into the dissolution of spray-dried amorphous solid dispersions. *J Pharm Sci* 2012;8:2798–810.
- Pereira JM, Mejia-Ariza R, Ilevbare GA, et al. Interplay of degradation, dissolution and stabilization of clarithromycin and its amorphous solid dispersions. *Mol Pharm* 2013;12:4640–53.
- Sun Y, Zhu L, Wu T, et al. Stability of amorphous pharmaceutical solids: crystal growth mechanisms and effect of polymer additives. *Aaps J* 2012;3:380–8.
- Ganesan P, Soundararajan R, Shanmugam U, Ramu V. Development, characterization and solubility enhancement of comparative dissolution study of second generation of solid dispersions and microspheres for poorly water soluble drug. *Asian J Pharm Sci* 2015;5:433–41.

7. Andrews GP, Abudiak OA, Jones DS. Physicochemical characterization of hot melt extruded bicalutamide–polyvinylpyrrolidone solid dispersions. *J Pharm Sci* 2010;3:1322–35.
8. Chan S-Y, Chung Y-Y, Cheah X-Z, et al. The characterization and dissolution performances of spray dried solid dispersion of Ketoprofen in hydrophilic carriers. *Asian J Pharm Sci* 2015;5:372–85.
9. Vo CL-N, Park C, Lee B-J. Current trends and future perspectives of solid dispersions containing poorly water-soluble drugs. *Eur J Pharm Biopharm* 2013;3:799–813.
10. Karavas E, Georgarakis E, Sigalas MP, et al. Investigation of the release mechanism of a sparingly water-soluble drug from solid dispersions in hydrophilic carriers based on physical state of drug, particle size distribution and drug-polymer interactions. *Eur J Pharm Biopharm* 2007;3:334–47.
11. Stewart PJ, Zhao F-Y. Understanding agglomeration of indomethacin during the dissolution of micronised indomethacin mixtures through dissolution and de-agglomeration modeling approaches. *Eur J Pharm Biopharm* 2005;2:315–23.
12. Kapsi SG, Ayres JW. Processing factors in development of solid solution formulation of itraconazole for enhancement of drug dissolution and bioavailability. *Int J Pharm* 2001; 229:193–203.
13. Kestur US, Ivanovic I, Alonzo DE, Taylor LS. Influence of particle size on the crystallization kinetics of amorphous felodipine powders. *Powder Technol* 2013;236:197–204.
14. Bruce C, Fegely KA, Rajabi-Siahboomi AR, McGinity JW. Crystal growth formation in melt extrudates. *Int J Pharm* 2007;341:162–72.
15. Jijun F, Lishuang X, Xiaoguang T, et al. The inhibition effect of high storage temperature on the recrystallization rate during dissolution of nimodipine–Kollidon VA64 solid dispersions (NM–SD) prepared by hot-melt extrusion. *J Pharm Sci* 2010; 5:1643–7.
16. Gupta MK, Tseng Y-C, Goldman D, Bogner RH. Hydrogen bonding with absorbent during storage governs drug dissolution from solid-dispersion granules. *Pharm Res* 2002; 11:1663–71.
17. Ghebremeskel A, Vemavarapu C, Lodaya M. Use of surfactants as plasticizers in preparing solid dispersions of poorly soluble API: stability testing of selected solid dispersions. *Pharm Res* 2006;8:1928–36.
18. Sharma A, Jain CP, Tanwari YS. Preparation and characterization of solid dispersion of carvedilol with poloxamer 188. *J Chil Chem Soc* 2013;1:1553–7.
19. Song Y, Wang L, Yang P, et al. Physicochemical characterization of felodipine-kollidon VA64 amorphous solid dispersions prepared by hot-melt extrusion. *J Pharm Sci* 2013;6:1915–23.
20. Wegiel L, Mosquera-Giraldo L, Mauer L, et al. Phase behavior of resveratrol solid dispersions upon addition to aqueous media. *Pharm Res* 2015;32:3324–37.
21. Chauhan H, Hui-Gu C, Atef E. Correlating the behavior of polymers in solution as precipitation inhibitor to its amorphous stabilization ability in solid dispersions. *J Pharm Sci* 2013; 6:1924–35.
22. Mirza S, Miroshnyk I, Habib MJ, et al. Enhanced dissolution and oral bioavailability of piroxicam formulations: modulating effect of phospholipids. *Pharmaceutics* 2010;4:339–50.
23. Kakran M, Sahoo NG, Li L. Dissolution enhancement of quercetin through nanofabrication, complexation, and solid dispersion. *Colloids Surf B Biointerfaces* 2011;1:121–30.
24. Syed HK, Liew KB, Loh GOK, Peh KK. Stability indicating HPLC–UV method for detection of curcumin in curcuma longa extract and emulsion formulation. *Food Chem* 2015; 170:321–6.
25. Viegas TX, Curatella RU, Winkle LLV, Brinker G. Measurement of intrinsic drug dissolution rates using two types of apparatus. *Pharm Technol* 2001;6:44–53.
26. Wu K, Li J, Wang W, Winstead DA. Formation and characterization of solid dispersions of piroxicam and polyvinylpyrrolidone using spray drying and precipitation with compressed antisolvent. *J Pharm Sci* 2009;98:2422–31.
27. Chan S-Y, Qi S, Craig DQM. An investigation into the influence of drug–polymer interactions on the miscibility, processability and structure of polyvinylpyrrolidone-based hot melt extrusion formulations. *Int J Pharm* 2015;1:95–106.
28. Rahman Z, Bykadi S, Siddiqui A, Khan MA. Comparison of X-ray powder diffraction and solid-state nuclear magnetic resonance in estimating crystalline fraction of tacrolimus in sustained-release amorphous solid dispersion and development of discriminating dissolution method. *J Pharm Sci* 2015;5:1777–86.
29. Patel BB, Patel JK, Chakraborty S, Shukla D. Revealing facts behind spray dried solid dispersion technology used for solubility enhancement. *Saudi Pharm J* 2015;4:352–65.
30. Wegiel LA, Mauer LJ, Edgar KJ, Taylor LS. Crystallization of amorphous solid dispersions of resveratrol during preparation and storage—Impact of different polymers. *J Pharm Sci* 2013;1:171–84.
31. Jørgensen AC, Torstenson AS. Humid storage conditions increase the dissolution rate of diazepam from solid dispersions prepared by melt agglomeration. *Pharm Dev Technol* 2008;3:187–95.
32. Newman A, Knipp G, Zograf G. Assessing the performance of amorphous solid dispersions. *J Pharm Sci* 2012;4:1355–77.
33. Tres F, Treacher K, Booth J, et al. Real time Raman imaging to understand dissolution performance of amorphous solid dispersions. *J Control Release* 2014;188:53–60.
34. Lu Y, Tang N, Lian R, et al. Understanding the relationship between wettability and dissolution of solid dispersion. *Int J Pharm* 2014; 465:25–31.